J. Phys. Chem. A **2000,** *104,* 3481−3486

Matrix Isolation Investigation of the Interaction of SiH_4 with NH_3 and $(CH_3)_3N$[†]

Daniel R. Meininger and Bruce S. Ault*

Department of Chemistry, University of Cincinnati, P.O. Box 210172, Cincinnati, Ohio 45221

Received: September 2, 1999; In Final Form: November 9, 1999

Co-deposition of samples of SiH_4 and NH_3 or the methylamines into argon and nitrogen matrices has led to the first isolation and characterization of 1:1 complexes between these reactants. Several Si−H stretching modes were observed, shifted as a result of complex formation. The Si−H axial stretch, in particular, shifted to lower energy upon complexation, with a shift that increased monotonically with the intrinsic basicity of the amine. The symmetric deformation mode of the complexed NH_3 subunit shifted to higher energy, and retained evidence of hindered rotation about its C_3 axis in solid argon, but not in solid nitrogen. The shifts of these vibrational modes were in good agreement with previous ab initio calculations, as well as calculations performed here. All of the spectral evidence points to a very weak binding energy in these complexes, in agreement with calculations.

Introduction

Many substituted silanes, particularly halogenated silanes, function as Lewis acids in a range of chemical reactions.[1] As a consequence of this Lewis acidity, these silanes form stable adducts with electron donors. For example, the 1:2 adduct of SiF_4 with NH_3 is well known and characterized.[2,3] 1:1 Adducts are generally less well known, except for sterically hindered Lewis acids.[4] However, adducts of the simplest silane, SiH_4, with electron donors have not been reported to date, although vapor pressure data[5] have been interpreted to indicate the formation of an adduct between SiH_4 and $(CH_3)_3N$. Several theoretical calculations have studied the interaction between SiH_4 and NH_3, and the two most recent studies[6,7] have concluded that this adduct should be stable and observable, albeit weakly bound.

The matrix isolation technique[8−10] was developed for the isolation and characterization of reactive chemical intermediates, including radicals, ions, and weakly bound molecular complexes. This technique was successfully employed to provide the first definitive evidence for the 1:1 complex $SiF_4·NH_3$, a species found to be trigonal bipyramidal, with the NH_3 ligand in an axial position.[11] Several subsequent theoretical studies have confirmed this structure.[7] While this adduct is calculated to be more strongly bound than the analogous SiH_4 adduct, matrix isolation provides the most likely route to the synthesis and characterization of the adduct between SiH_4 and NH_3. In view of the importance of SiH_4 and the interest in its chemistry, a study was undertaken to explore the interaction of SiH_4 with NH_3 and with the methylamines.

Experimental Section

All of the experiments in the current study were carried out on conventional matrix isolation apparatus that has been described.[12,13] Silane samples were prepared from a commercial 1% mixture of SiH_4 in argon (Matheson). For argon matrix experiments, this mixture was diluted with additional argon to the desired ratio. For nitrogen matrix experiments, the SiH_4 was separated from the argon by fractional distillation at 77 K, and the matrix sample prepared by dilution to the desired ratio in N_2. NH_3, CH_3NH_2, $(CH_3)_2NH$ and $(CH_3)_3N$ (all Matheson) as well as $^{15}NH_3$ (Cambridge Isotope Laboratory, 99% ^{15}N) and $(CD_3)_3N$ (Merck, 99% D) were all introduced into the vacuum system as gases from lecture bottles and were purified by freeze−pump−thaw cycles at 77 K. Argon and nitrogen (Wright Brothers) were used as the matrix gases in different experiments, and were used without further purification.

Samples of SiH_4 and NH_3 in the appropriate matrix gas were deposited from separate vacuum manifolds onto the 14 K cold window in either the twin jet or the merged jet mode. In the former, the two samples are deposited simultaneously from two different nozzles onto the cryogenic surface, with only a very brief mixing time during the deposition process. In the latter, the two gas deposition lines are joined by an Ultratorr tee at a chosen distance from the cryogenic surface. The two gas samples then flow together through the remaining length of tubing, typically 50−100 cm, allowing for increased mixing and reaction time relative to twin jet deposition. Samples were deposited for 20−24 h at 2 mmol/hr for each gas sample. Final spectra were recorded on a Nicolet IR42 at 1 cm^{-1} resolution, over the range 4000−400 cm^{-1}. A number of samples were then annealed gently to between 25 and 30 K, recooled to 14 K and additional spectra were recorded.

Results

Prior to any co-deposition experiments, blank experiments were conducted on each reagent in both argon and nitrogen matrices. In each case, the resulting spectra were in good agreement with literature spectra,[14−18] and with spectra recorded previously in this laboratory. Reference matrices for each reagent in each matrix were also annealed to as high as 30 K and recooled and additional spectra recorded. Some changes were noted in the spectra and were indicative of increased aggregation, particularly dimerization, of the reagent.

SiH_4 + NH_3. In an initial merged jet experiment, a sample of Ar/NH_3 was co-deposited with a sample of Ar/SiH_4. Six new spectral features were observed, all rather weak, at 898, 982, 984, 1004, 2154, and 2225 cm^{-1}, in addition to a possible new feature at 2186 cm^{-1}. While this last band overlapped a very intense band of parent SiH_4, it was nonetheless distinct. The

---

[†] Part of the special issue “Marilyn Jacox Festschrift”.

10.1021/jp9931253 CCC: $19.00

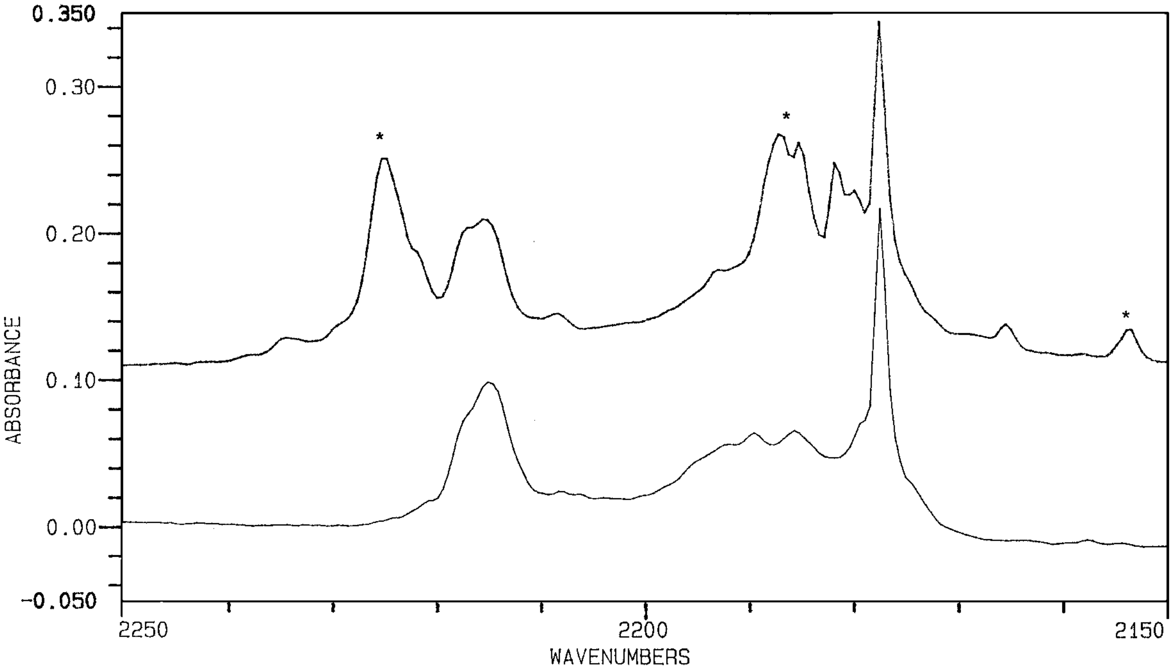

Figure 1. Infrared spectrum between 2150 and 2250 cm^{-1} of the matrix resulting from the co-deposition of a sample of Ar/SiH_4 with a sample of Ar/NH_3 (upper trace) compared to the spectrum of a sample of Ar/SiH_4 at 14 K. Bands marked with an asterisk (*) are due to the $SiH_4 \cdot NH_3$ complex.

others, while weak, were relatively well defined. A number of subsequent experiments were then carried out, over a wide range of sample concentrations (from $Ar/SiH_4 = 1000$ to $Ar/SiH_4 = 30{,}000$ and $Ar/NH_3 = 100$ to $Ar/NH_3 = 1000$). In all of these experiments, the same set of new bands was seen, and the bands in this set all maintained approximately a constant intensity ratio with respect to one another. Further, no additional bands were seen, other than those of dimers and higher oligomers of NH_3, which were also seen in spectra of reference matrices. The product band at 2186 cm^{-1} was most apparent when very low levels of SiH_4 were employed, as can be seen in Figure 1. When argon matrices containing SiH_4 and NH_3 were annealed in several different experiments, the weak new bands described above all *decreased* in intensity, while aggregate features of the parent molecules (particularly bands due to the NH_3 dimer) grew in intensity, as they did in the blank experiments. Several twin jet experiments were also conducted with this pair of reagents, at different sample concentrations. The spectra of matrices deposited using twin jet deposition were identical to those formed using merged jet deposition. This indicates that reaction is occurring only on the surface of the depositing matrix, and not during passage through the merged region, in the merged jet experiments.

NH_3 is known[15] to undergo hindered rotation in argon matrices, leading to complexities in the spectral regions near the fundamentals of NH_3. It is also known[16] that such motions do not take place in N_2 matrices, leading to much simpler spectra. Therefore, a number of experiments were conducted in which samples of N_2/SiH_4 were co-deposited with samples of N_2/NH_3. In all of these experiments, four distinct new absorptions were noted in the resultant spectra, at 898, 994, 2175, and a doublet 2212, 2216 cm^{-1}. Just as in the argon matrix experiments, these bands were reproducible over a range of sample concentrations, and the bands maintained a constant intensity ratio with respect to one another, within the uncertainty of the intensity measurements. One additional band, at 2161 cm^{-1}, was seen in some experiments, typically when the NH_3 concentration was high relative to SiH_4. Several of these N_2 matrices were then annealed to around 30 K and recooled. The resultant spectra showed that the bands at 898, 994, 2175, and 2214 cm^{-1} all decreased in intensity, while the band at 2161 cm^{-1} increased somewhat.

A similar series of experiments was conducted using $^{15}NH_3$ and SiH_4, with deposition into both argon and N_2 matrices. In argon, analogous product bands were observed at 898, 977, 980, 1000, 2186, and 2225 cm^{-1}, with the same relative intensities and annealing behavior as described above for the $^{14}NH_3$ experiments. No additional product bands were observed, although there was some residual $^{14}NH_3$ in the $^{15}NH_3$ experiments, and the ^{14}N product bands were very weakly observed. The results in N_2 matrices were very similar, with product bands at 898, 990, and the doublet at 2212, 2216 cm^{-1}. Figure 2 shows the spectrum of such a matrix, in the region of the symmetric deformation of NH_3. Table 1 lists all of the product bands for the SiH_4/NH_3 system.

SiH_4 + Methylamines. In an extensive series of experiments, SiH_4 was co-deposited with $(CH_3)_3N$ and $(CD_3)_3N$ into both argon and N_2 matrices, and less extensively with $(CH_3)_2NH$ and CH_3NH_2. In these experiments, argon matrices gave the sharper, more definitive spectra. With $(CH_3)_3N$, product bands were observed at 818, 902, 982, 1193, 2111, and 2174 cm^{-1}. Of these, the 2111 cm^{-1} band was the sharpest and most distinctive, while the band at 982 cm^{-1} was particularly broad and weak. In the N_2 matrix experiments, bands were observed near 818, 985, 1193, and 2115 cm^{-1}, all broadened substantially compared to the argon matrix results. Co-deposition of SiH_4 with $(CD_3)_3N$ into argon matrices led to similar results, with shifting of certain of the product bands, and not of others. Product bands were observed at 735, 902, 982, 1010, and 2108 cm^{-1}, again with the 2108 cm^{-1} band being the sharpest and the 982 cm^{-1} band being particularly broad. N_2 matrix experiments led to a broadening of these product bands, just as was noted with the normal isotope. Table 2 lists all of the product bands for the $SiH_4/(CH_3)_3N$ system.

Experiments were conducted also with mono- and dimethylamine, with a focus on the Si–H stretching region. In the co-

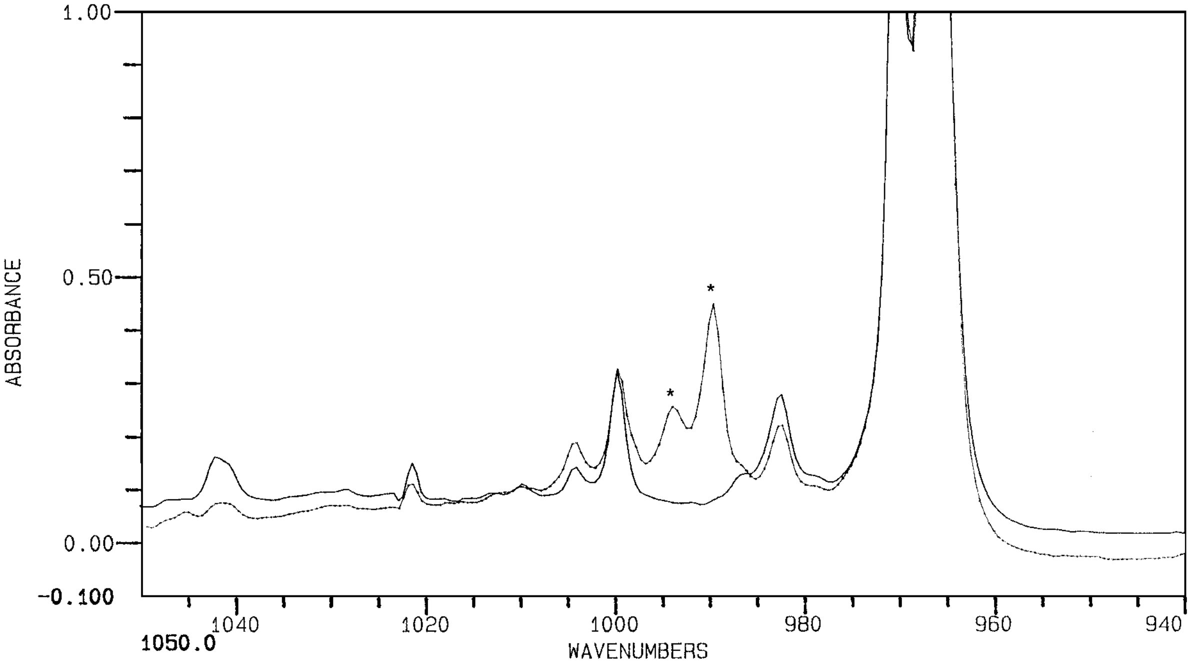

Figure 2. Infrared spectrum, between 940 and 1050 cm^{-1}, of a sample of $N_2/^{14,15}NH_3$ (lower trace) at 14 K compared to the spectrum of a sample of $N_2/SiH_4/^{14,15}NH_3$, also at 14 K (upper trace). The bands marked with an asterisk (*) are product bands due to the symmetric deformation modes of $^{14}NH_3$ and $^{15}NH_3$, respectively, complexed with SiH_4.

TABLE 1: Band Positions[a] and Assignments for the 1:1 Complex $SiH_4 \cdot NH_3$ in Argon Matrices

$SiH_4 \cdot {}^{14}NH_3$ (cm^{-1})	$SiH_4 \cdot {}^{15}NH_3$ (cm^{-1})	assignment
898 (898)	898 (898)	SiH_4 antisym. deform.
982 (994)	977 (990)	NH_3 sym. deform. $Q(1^+{}_1)^b$
984	980	NH_3 sym. deform. $P(1^+{}_0)$
1004	1000	NH_3 sym. deform. $R(0^-{}_0)$
2154 (2175)	–	$Si{-}H_{ax}$ stretch
2186	2186	$Si{-}H_{eq}$ stretch
2225 (2214)	2225 (2214)	$Si{-}H_{eq}$ stretch

[a] Band positions given in parentheses are nitrogen matrix values; hindered rotation does not occur in N_2, so only the Q branch is observed. [b] Notation from ref 15.

TABLE 2: Band Positions[a] and Assignments for the 1:1 Complex $SiH_4 \cdot N(CH_3)_3$ in Argon Matrices

$SiH_4 \cdot N(CH_3)_3$ (cm^{-1})	$SiH_4 \cdot N(CD_3)_3$ (cm^{-1})	assignment
818	735	NC_3 stretch
902	902	SiH_4 antisym. deform.
982 (985)	982	SiH_4 symmetic deform.
1193 (1193)	1010 (1010)	CH_3 rock
2111 (2115)	2108 (2108)	$Si{-}H_{ax}$ stretch
2174	–	$Si{-}H_{eq}$ stretch

[a] Band positions given in parentheses are nitrogen matrix values.

deposition experiments with CH_3NH_2, a sharp, distinct product band was observed in this region at 2151 cm^{-1} in an N_2 matrix. In the analogous experiment with $(CH_3)_2NH$, a comparable but shifted product band was noted at 2136 cm^{-1}. These bands are shown in Figure 3. These product bands were reproducible in the several experiments that were conducted with each pair of reagents.

Ab Initio Calculations. A number of calculations were carried out on the reagents in this study, and their possible 1:1 complexes, using the *Gaussian 94* suite of programs[19] at the restricted Hartree−Fock (RHF) level of theory. A number of basis sets were employed, from the 6-31G* to the 6-31++-(2d,p) basis set. Relatively little variation of geometric parameter with basis set was noted, and results with the 6-31G+ (d′,p′) basis set are reported here. The goal of these calculations was to confirm the results of Rossi and Jasinski[6] (hereafter RJ) and to calculate frequencies and isotopic shifts for vibrational modes upon complexation for those isotopically labeled (^{15}N, ^2H) complexes not studied by RJ. Calculations on the $SiH_4 \cdot NH_3$ and $SiH_4 \cdot N(CH_3)_3$ complexes converged to stable minima, leading to all positive frequencies. The calculated structure of the $SiH_4 \cdot NH_3$ complex was similar to that calculated by RJ, except for a somewhat longer Si−N distance, as shown in Table 3. This apparent lengthening of the Si−N distance is probably a reflection of the flatness of the potential energy surface which, in turn, is a function of the very low binding energy for the complex. The vibrational frequency shifts from the parent reagents to the complex calculated in this study agree reasonably well with those of RJ, as shown in Table 4. Calculations on the $SiH_4 \cdot N(CH_3)_3$ complex were generally similar, leading to the structure shown in Table 5.

Discussion

Product Identification. The co-deposition of NH_3 with SiH_4 into argon and nitrogen matrices led to the observation of new infrared absorptions. Similar results were noted when the methylamines were employed. These observations indicate formation of a new absorbing species, one that is dependent on presence of both NH_3 and SiH_4. The new product bands were weak yet distinct and reproducible in a wide range of experiments. Moreover, the product bands for a given pair of reagents (e.g., the bands at 898, 982, 984, 1004, 2154, and 2225 cm^{-1} for SiH_4/NH_3 in argon) maintained a constant intensity ratio with respect to one another in a large number of experiments over a wide range of conditions. This is indicative of the formation of a single new product species (the only exception to this is the 2161 cm^{-1} band in the SiH_4/NH_3 system in nitrogen matrices, which did not show the same concentration dependence; see below for a discussion of this band).

The product bands observed in these systems were located quite near (within 50 cm^{-1}) a vibrational mode of one of the

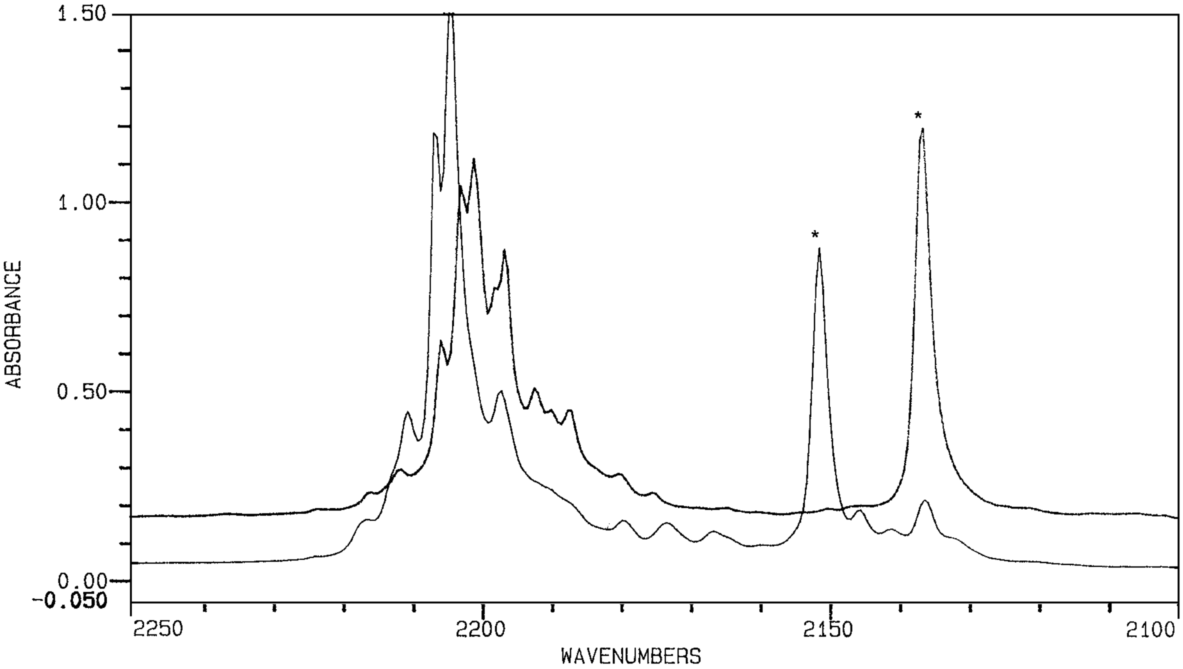

Figure 3. Infrared spectrum between 2100 and 2250 cm^{-1} of the matrix resulting from the co-deposition of a sample of N_2/CH_3NH_2 with a sample of N_2/SiH_4 (lower trace) compared to the spectrum of a matrix resulting from the co-deposition of a sample of $N_2/(CH_3)_2NH$ with a sample of N_2/SiH_4 (upper trace). Note that slight impurity $(CH_3)_2NH$ is always present in samples of CH_3NH_2, accounting for the weak band at 2136 cm^{-1} in the CH_3NH_2/SiH_4 experiment. Bands marked with an asterisk (*) are due to the Si−H axial stretch of the respective complexes with SiH_4.

TABLE 3: Ab Initio Structure of the $SiH_4 \cdot NH_3$ Complex

parameter	this work	Rossi and Jasinski[a]
point group	C_{3v}	C_{3v}
R (Si−H_{ax})	1.483 Å	1.473 Å
R (Si−H_{eq})	1.480	1.464
R (Si−N)	3.393	3.131
R (N−H)	1.001	1.014
α (H_{eq}-Si−N)	71.7°	72.6°
α (Si−N−H)	110.7°	111.9°

[a] Reference 6.

TABLE 4: Comparison of Experimental and Calculated Vibrational Frequency Shifts for the $SiH_4 \cdot NH_3$ Complex

mode	exptl shift (cm^{-1})	calc'd shift[b] (cm^{-1})	calc'd shift[c] (cm^{-1})
SiH_4 antisym. deform.	−2	−2	−9
NH_3 sym. deform.	+30	+36	+26
Si−H_{ax} stretch	−29[a]	−50	−28
Si−H_{eq} stretch	+9	+8	+8

[a] Derived from the symmetric stretch of parent SiH_4; parent band position taken from ref 26. [b] Rossi and Jasinski, ref 6. [c] This work.

TABLE 5: Calculated Structure Parameters for the 1:1 Complex $SiH_4 \cdot N(CH_3)_3$

parameter	calc'd value[a]	parent value[a]
R (Si−H_{ax})	1.485 Å	1.478 Å
R (Si−H_{eq})	1.478	1.478
R (Si−N)	3.216	−
R (N−C)	1.452	1.445
α (H_{ax}−Si−H_{eq})	107.8°	109.5°
α (H_{eq}−Si−H_{eq})	111.1°	109.5°

[a] Calculation employed RHF, with the 6-31G*(d,p) basis set, this work.

two reagents in the system. This is indicative of complex formation,[20] where each subunit in the complex is perturbed by the presence of the other subunit, rather than more extensive reaction with bond breaking and bond formation. This is particularly notable in the NH_3 symmetric deformation region in argon matrices, where the spectrum of the product retains the hindered rotational pattern observed for the parent,[15,16] with each component shifted about 30 cm^{-1} to higher energies (see below for detailed band assignments). It is also noteworthy that previous calculations[6,7] as well as those carried out here demonstrate that SiH_4 should form a weakly bound molecular complex with NH_3 and with the methylamines, i.e., that the complex represents a local minimum on the potential energy surface. Taken together, all of the above arguments support the identification of the new infrared absorber in these experiments as a molecular complex formed between SiH_4 and NH_3 or the respective methylamine. *This provides the first direct experimental evidence for the existence of these weakly bound species*. At the same time, the sharpness of the product absorptions indicate that, although weakly bound, these species have a well-defined structure.

The stoichiometry of the complex remains to be determined. While the calculations focused on the 1:1 complex, formation of higher complexes (e.g., 1:2) is possible as well. However, the concentrations employed in this study were very low, as dilute as 1/10,000 in some experiments. Under these conditions, it is hard to envision the formation of a complex of stoichiometry greater than 1:1. If a complex of higher stoichiometry were formed, then it is likely to occur through stepwise addition of a second molecule to the 1:1 complex. However, only a single product species was observed (except in the $SiH_4/NH_3/N_2$ system). Finally, the calculations performed by RJ and in the current study also predict the vibrational frequencies of the complex and shifts from the parent modes. While these will be discussed in more detail below, it can be noted here that the agreement between the observed band shifts and the calculated band shifts for the 1:1 complex is very good. All of these facts argue that the stoichiometry of the molecular complex formed in this study is 1:1. As a result, the new infrared absorptions observed here are assigned to the 1:1 molecular complex between SiH_4 and NH_3 or the appropriate methylamine.

The 2161 cm^{-1} band in the $SiH_4/NH_3/N_2$ system remains to be identified. This band is clearly due to a different absorber, based on concentration dependence and annealing behavior. In particular, this band was observed at high NH_3/SiH_4 ratios, and grew upon annealing, where higher aggregation can occur. Consequently, this band is best assigned to a complex of higher stoichiometry, $SiH_4\cdot(NH_3)_x$, with $x > 1$. While there is insufficient evidence to determine x conclusively, it is very likely that $x = 2$, and hence the bands are probably due to the 1:2 complex $SiH_4\cdot 2NH_3$.

Band Assignments. Since each of the product bands observed here was near a vibrational mode of one of the two subunits in the complex, assignment of the bands is relatively straightforward and is assisted further by the ab initio calculations. Complex formation by NH_3 is well known to lead to a blue shift of the symmetric deformation or "umbrella" mode of NH_3; the magnitude of this shift is often taken as an indicator of the strength of the interaction.[21] This mode lies near 970 cm^{-1} for the parent. In argon, hindered rotation around the C_3 axis has been observed and assigned[15] to a $Q(1^+_1)$ line at 956 cm^{-1}, a $P(1^+_0)$ line at 962 cm^{-1} (both weak), and a stronger $R(0^-_0)$ line at 970 cm^{-1}. In the present study, three bands in this region were noted, at 982, 984, and 1004 cm^{-1}, blue shifted 26, 22, and 30 cm^{-1}, respectively. These are assigned to hindered rotational structure on the symmetric deformation mode, with a slight change in the hindered rotation due to complex formation. In N_2 matrices, only a single sharp line was observed, at 994 cm^{-1}, blue shifted 24 cm^{-1} from the intense parent mode at 970 cm^{-1}. Confirmation of these assignments comes from the 4 cm^{-1} shift observed for each of these product bands upon ^{15}N substitution. This shift is identical to that observed for this mode of parent NH_3. Finally, the ab initio calculations of RJ predict a 36 cm^{-1} blue shift, while the current calculations predict a 26 cm^{-1} blue shift, both in good agreement with the observed values.

Three product bands fell in the region between 2100 and 2250 cm^{-1}, attributable to Si−H stretching modes. The parent mode of SiH_4 in this region is triply degenerate yet appears broad and split into two maxima, at 2177 and 2215 cm^{-1}. Earlier studies[14,22] have speculated on different environments or sites within the matrix, without definitive conclusion. This is consistent with the annealing behavior observed here, where the 2215 cm^{-1} band decreased upon annealing, while the 2177 cm^{-1} band increased. The two most distinct product bands were at 2154 and 2225 cm^{-1}. In addition, in experiments with low SiH_4 concentration, a band at 2186 cm^{-1} was seen on the high energy side of the intense 2177 cm^{-1} parent band. Upon complex formation, the symmetric stretch of the SiH_4 subunit must be lowered, to at least C_{3v}. RJ computationally explored different structural arrangements of the complex, and determined that in the lowest energy structure the NH_3 subunit approaches the Si atom along a C_3 axis, leading to an incipient trigonal bipyramidal structure with C_{3v} symmetry. This is also the structure determined experimentally[11] and theoretically[7,23] for the analogous complex $SiF_4\cdot NH_3$.

Under C_{3v} symmetry the F_2 mode splits into an A_1 and an E mode, while the totally symmetric A_1 mode is activated. The former modes become the symmetric and antisymmetric stretching modes of the three equivalent (incipient) equatorial hydrogens, while the last mode transforms into the Si−H stretch of the axial Si−H bond. The antisymmetric equatorial stretching mode is calculated to shift to the blue by 8 cm^{-1}, while the symmetric equatorial stretch is predicted to shift by only 2 cm^{-1}, and to have very low intensity. On the other hand, the Si−H axial stretch is calculated to have a significant red shift (25−50 cm^{-1}) and be moderately intense. Based on these observations, the 2225 cm^{-1} band is assigned to the equatorial antisymmetric stretch of SiH_4 in the 1:1 complex, blue shifted 10 cm^{-1} from the site-split parent band at 2215 cm^{-1}, while the 2186 cm^{-1} band is assigned to the same mode in the complex blue shifted 9 cm^{-1} from the site-split parent band at 2177 cm^{-1}. The 2154 cm^{-1} band is assigned to the Si−H axial stretch, red shifted from the infrared inactive parent mode, which has been identified at 2180 cm^{-1} in Raman spectra. This red shift of 29 cm^{-1} is in good agreement with the calculated shift of RJ and the present calculations, as shown in Table 4. N_2 matrices present a different environment, and led to the observation of the antisymmetric equatorial Si−H stretch at 2214 cm^{-1} and the Si−H axial stretch at 2175 cm^{-1}.

TABLE 6: Position of the Si−H_{ax} Stretching Mode of SiH_4·Amine Complexes in N_2 Matrices

base	Si−H_{ax} stretch (cm^{-1})	PA[a] (cm^{-1})
NH_3	2175	207
CH_3NH_2	2151	216
$(CH_3)_2NH$	2136	222
$(CH_3)_3N$	2111	227

[a] Proton affinity of the base, in kcal/mol, from ref 23.

The $SiH_4\cdot N(CH_3)_3$ complex in argon matrices had two bands in the Si−H stretching region, at 2111 and 2174 cm^{-1}. The former had a nitrogen matrix counterpart at 2115 cm^{-1}, while the N_2 matrix counterpart of the latter band was not observed, and probably hidden under the intense parent band. Calculations and comparison to similar systems suggest that the antisymmetric equatorial stretch should shift only slightly with a change in base, while the Si−H axial stretch which is trans to the coordinated base should shift strongly to lower energy with an increasing base strength. Thus, the Si−H equatorial stretch is anticipated in the range 2170−2190 cm^{-1}, while the Si−H axial stretch is anticipated below the 2154 cm^{-1} position for the $SiH_4\cdot NH_3$ complex in argon matrices. Also, the 2111 cm^{-1} band showed a 3 cm^{-1} red shift when $N(CD_3)_3$ was employed, to 2108 cm^{-1}. Mechanical coupling of this heavier mass to the Si−H axial stretch would be expected to lead to a small red shift, while mechanical coupling to the equatorial Si−H oscillators is not expected to occur. The observation of a red shift, combined with the above arguments, led to the assignment of the 2174 cm^{-1} band to the Si−H antisymmetric equatorial stretch and the 2111 cm^{-1} band to the Si−H axial stretch in the 1:1 complex $SiH_4\cdot N(CH_3)_3$.

Experiments in which $(CH_3)_2NH$ and CH_3NH_2 were codeposited with SiH_4 focused on the Si−H stretching region. For each base, one distinct, sharp band was observed, at 2151 cm^{-1} with CH_3NH_2 and 2136 cm^{-1} with $(CH_3)_2NH$, *both in* N_2 *matrices*. These may be assigned to the Si−H axial stretch in these complexes with bases of intermediate base strength (between NH_3 and $(CH_3)_3N$). Table 6 lists the position of the Si−H axial stretching mode for each of the four complexes observed here, as a function of the proton affinity of the base.[23] As can be seen, the magnitude of the red shift of the Si−H axial stretch increases monotonically with increasing intrinsic base strength of the amines.

The bending modes of parent SiH_4 transform as an infrared forbidden (in T_d symmetry) E mode and an infrared active F_2 mode. The spectra of the $SiH_4\cdot NH_3$ and $SiH_4\cdot N(CH_3)_3$ complexes each contained a weak band near 900 cm^{-1}, slightly to the blue of the intense parent F_2 bending mode. This band, in the case of the $(CH_3)_3N$ complex, did not shift upon deuteration, indicating that it is due to a vibrational mode of the SiH_4 subunit in the complex. In view of the proximity to the F_2 mode of the parent, this band is assigned as an antisymmetric bending mode of the SiH_4 subunit in the 1:1 complex. Also, in the $(CH_3)_3N$ and $(CD_3)_3N$ complexes with SiH_4, a weak broad band was seen near 982 cm^{-1}. This lies very near the infrared inactive SiH_4 bending mode of *E* symmetry, and is tentatively assigned to this mode, perturbed and activated in the complex.

Just as the acceptor in the complex is perturbed upon complexation, so also is the base, as described above for the NH_3 subunit in the $SiH_4{\cdot}NH_3$ complex. As noted in Table 2, two additional product bands were observed in the spectrum of the $SiH_4{\cdot}N(CH_3)_3$ and $SiH_4{\cdot}N(CD_3)_3$ complexes. For both systems, one was near the NC_3 stretching mode of the trimethylamine subunit and one was near a CH_3 rocking mode. Based on their proximity to the analogous parent bands, they are assigned to the same modes of the perturbed trimethylamine subunit in the 1:1 complex.

Further Considerations. The shift of the symmetric deformation mode of NH_3 in a molecular complex is often taken as indicative of the strength of interaction in the complex.[20,21] The shift here, 30 cm^{-1}, is very small. For comparison, a shift as large as 343 cm^{-1} has been reported in the strongly bound $NH_3{\cdot}SO_3$ complex,[24] and as small as 64 cm^{-1} in the weakly bound $NH_3{\cdot}SO_2$ complex[25] (of course, the NH_3 dimer shows shifts of 35−65 cm^{-1} also). This result is consistent with the very small binding energy, 2.61 kcal/mol, calculated by RJ, and with the previous lack of observation of this species.

As noted above, the position of the Si−H axial stretch is dependent upon the base subunit in the complex. The stronger the base, given by the gas phase proton affinity, the greater the shift in this mode, and presumably the stronger the interaction. Thus, while these complexes are all weakly bound, addition of methyl groups to the base does detectably alter the binding energy and the infrared spectrum. This is consistent with the fact that the existence a of complex between SiH_4 and $(CH_3)_3N$, the strongest base studied here, has been inferred from vapor pressure data above a solution of these two reactants.[5]

An unusual feature of the current experiments is the behavior of the product bands upon annealing. Generally, bands due to molecular complexes grow upon annealing, as limited diffusion through the matrix material permits acid−base encounters and allows for additional complex formation. However, the product bands here decreased upon annealing to 25 K and recooling to 12 K. One possible explanation for this behavior is that the interaction energy between NH_3 units to form the dimer or higher oligomers (which were observed to grow) is greater than the strength of interaction between SiH_4 and NH_3. Thus, the NH_3 molecules prefer to associate with other NH_3 molecules, rather than SiH_4 (a form of phase separation within the argon matrix). While this cannot be determined conclusively, this does not counter the above arguments in support of the identification and characterization of these novel molecular complexes.

Acknowledgment. The authors gratefully acknowledge the National Science Foundation for support of this research through grants CHE93-22622 and CHE98-77076.

References and Notes

(1) Jensen, W. B, *The Lewis Acid−Base Concepts, an Overview*; Wiley-Interscience: New York, 1980.

(2) Davy, J. *Philos. Trans. R. Soc. London* **1812**, 352.

(3) Porritt, C. J. *Chem. Ind. (London)* **1979**, 215.

(4) Beattie, I. R.; Ozin, G. A. *J. Chem. Soc. A* **1970**, 158.

(5) Watkins, J. J.; Sefcik, M. D.; Ring, M. A. *Inorg. Chem*. **1972**, *11*, 3146.

(6) Rossi, A. R.; Jasinski, J. M. *Chem. Phys. Lett*. **1990**, *169*, 399.

(7) (a) Gordon, M. S.; Davis, L. P.; Burggraf, L. W. *Chem. Phys. Lett*. **1989**, *163*, 371. (b) Marsden, C. J. *Inorg. Chem*. **1983**, *22*, 3178.

(8) Craddock, S.; Hinchliffe, A. *Matrix Isolation*; Cambridge University Press: Cambridge, 1975.

(9) Hallam, H. E. *Vibrational Spectroscopy of Trapped Species*; John Wiley: New York, 1973.

(10) Andrews, L.; Moskovitz, M., Eds. *Chemistry and Physics of Matrix Isolated Species*; Elsevier Science Publishers: Amsterdam, 1989.

(11) Ault, B. S. *Inorg. Chem*. **1981**, *20*, 2817.

(12) Ault, B. S. *J. Am. Chem. Soc*. **1978**, *100*, 2426.

(13) Carpenter, J. D.; Ault, B. S. *J. Phys. Chem.* **1991**, *95*, 3502.

(14) Wilde, R. E.; Srinivasan, T. K. K.; Harral, R. W.; Sankar, S. G. *J. Chem. Phys*. **1971**, *55*, 5681.

(15) Abouaf-Marguin, L.; Jacox, M. E.; Milligan, D. E. *J. Mol. Spectrosc.* **1977**, *67*, 34.

(16) Nelander, B. *Chem. Phys.* **1984**, *87*, 283.

(17) Goldfarb, T. D.; Khare, B. N. *J. Chem. Phys*. **1967**, *46*, 3379.

(18) Purnell, C. J.; Barnes, A. J.; Suzuki, S.; Ball, D. F.; Orville-Thomas, W. J. *Chem. Phys*. **1976**, *12*, 77.

(19) *Gaussian 94*, rev. E.1, Frisch, M. J.; Trucks, G. W.; Schlegel, H. B.; Gill, P. M. W.; Johnson, B. G.; Robb, M. A.; Cheeseman, J. R.; Keith, T.; Petersson, G. A.; Montgomery, J. A.; Raghavachari, K.; Al-Laham, M. A.; Zakrzewski, V. G.; Ortiz, J. V.; Foresman, J. B.; Cioslowski, J.; Stefanov, B. B.; Nanayakkara, M.; Challacombe, M.; Peng, C. Y.; Ayala, P. Y.; Chen, W.; Wong, M. W.; Andres, J. L.; Binkley, J. S.; Defrees, D. J.; Baker, J.; Stewart, J. P.; Head-Gordon, M.; Gonzalez, C.; Pople, J. A. Gaussian, Inc.: Pittsburgh, PA, 1995.

(20) Ault, B. S. *Rev. Chem. Intermed.* **1988**, *9*, 233.

(21) Nakamoto, K. *Infrared and Raman Spectroscopy of Inorganic and Coordination Compounds*, 5th ed.; Wiley-Interscience, New York, 1997.

(22) Davis, S. R.; Andrews, L. *J. Chem. Phys*. **1987**, *86*, 3765.

(23) Henderson, W. G.; Taagepera, M.; Holtz, D.; McIver, R. T., Jr.; Beauchamp, J. L.; Taft, R. W. *J. Am. Chem. Soc*. **1972**, *94*, 4728.

(24) Sass, C. S.; Ault, B. S. *J. Phys. Chem*. **1986**, *90*, 1547.

(25) Sass, C. S.; Ault, B. S. *J. Phys. Chem*. **1984**, *88*, 432.

(26) Herzberg, G. *Molecular Spectra and Molecular Structure, Vol. 2, Infrared and Raman Spectra of Polyatomic Molecules*; Van Nostrand: Princeton, NJ, 1945.